

# Design and Implementation of Real-time Fault Location Experimental System for Teaching and Training University Students

Case Study

## Ngo Minh Khoa

Quy Nhon University,  
Faculty of Engineering and Technology  
170 An Duong Vuong, Quy Nhon city, Vietnam  
ngominhkhoa@qnu.edu.vn

## Doan Duc Tung

Quy Nhon University,  
Faculty of Engineering and Technology  
170 An Duong Vuong, Quy Nhon city, Vietnam  
doanductung@qnu.edu.vn

**Abstract** – The fault location problem is one of the most important issues in power system operation and control. To obtain an experimental system for teaching and training electrical engineering students, this paper performed a study to design and implement a real-time fault location laboratory-scale model from practical hardware components. The impedance-based fault location method is embedded in the system to determine the distance to fault in the transmission line. Furthermore, the monitoring and controlling program is designed by the Matlab App Designer – A new professional app to create the graphical user interface and use the integrated editor quickly. Several fault types including three-phase fault, phase-to-phase fault, phase-to-ground fault are created to evaluate the performance of the fault location experimental system. The real-time measurement results which are acquired and observed on the user guide interface of the program confirm the effectiveness of the experimental system; therefore, the system can be considered a powerful tool for electrical engineering students.

---

**Keywords:** fault location, impedance method, transmission line, communication protocols, Matlab App Designer

---

## 1. INTRODUCTION

Power transmission lines play a crucial role in a power system. They are used to connect power stations and substations, and for connections between substations as well. They aim to efficiently transmit large amounts of power energy at high voltages [1-3]. Depending on the voltage level, the transmission line has different characteristics, i.e., long distances. Although a short circuit rarely occurs during a power system operation process, it is one of the most extremely serious errors. A short circuit is caused by many different sources and has a lot of effect on the power system [4-6], such as blackout, instability, interruption, etc.

Several methods have been developed to locate the fault in transmission and distribution lines [7-11]. The method based on reactance measurement has been proposed to locate a fault on overhead transmission lines of alternating current electrified railway [12]. Ref. [13] proposed the least-square method based on im-

pedance to locate a fault in the ungrounded grids. In Ref. [14], the impedance-based method was modified for estimating the distance to the fault in transmission lines in the presence of the fault current limiting. On the other hand, the travelling-based fault location methods have been proposed for estimating the fault location in the distribution network, such as the unsynchronized- and synchronized-based methods [15-19], the adaptive convolution neural network-based method [20, 21], and the single-end traveling wave fault location method [17, 22, 23]. For hybrid distribution lines, the authors in [24] proposed the single-ended fault location method based on the characteristic distribution of traveling wave along the transmission line.

For universities, electrical engineering students need to improve their knowledge about the fault location system for power transmission lines. Due to cost and space requirements as well as the complexity of a practical power system, the university students have less chance to interact with a practical power system

to study and verify the theory that they learned in the lectures. Therefore, laboratory experiments are one of the best approaches to link the theory with the hands-on skills of the students. For most students, laboratories are their first practical experiences and their excellent chances for not only achieving optimum learning experiences, but also developing valuable skills for future employment. Besides, the university can improve the quality of training of future electrical engineers by promoting their creativity and self-learning. One of the most important subjects for electrical engineering students is the relay protection in power system. The lessons of this subject are designed to help the students answering the following questions: "Which main components are included in a fault location system on transmission line?"; "Which signals from the measurement devices are applied for locating fault?"; "How does the fault location system response when a fault occurs in the transmission line?"; "How can the system detect and identify accurately the fault location on the transmission line?"; etc. These above teaching questions can be answered via the simulation programs such as: EMTP, Matlab/Simulink programs, etc.; however, the biggest limited issue of these simulation programs is the measurement data and control signals not in real-time. To help student get more theoretical and practical knowledge about the fault location system, the main objective of this paper is to design and implement a real-time fault location laboratory-scale system for a power transmission line supplying a load via only one source. This experimental system is built using hardware devices of the authors' smart grid laboratory for university students. In addition, its software is programmed on the Matlab platform for detecting, identifying, and locating faults which occur in a power transmission line.

## 2. DESIGN AND IMPLEMENTATION OF EXPERIMENTAL SYSTEM

### 2.1. HARDWARE UNIT

In a laboratory range, with a safety low voltage 380/220 V, the paper designs an experimental system based on the hardware components for locating faults in a power transmission line as shown in Fig. 1. The hardware devices in Fig. 1a consist of an adjustable three-phase power supply, a type- $\pi$  transmission line module, a load module, two power quality meters, a switch unit. These devices are available in the authors' smart grid laboratory, so students can easily access them to carry out various experiments for the designed system. Moreover, the personal computer, which is communicated to the devices (the two meters and two circuit breakers) via the Ethernet protocol, is used to represent the monitoring and controlling center. The algorithm for detecting, identifying, and locating faults on the transmission line is implemented on this computer and is run in real-time. The main specifications of the other hardware components in the experimental system are described as follows:

Firstly, the adjustable three-phase power supply is a voltage source which can adjust its output voltage in a range from 0 to 450V line-to-line voltage. This device is manufactured by Lucas Nuller, Germany. Its current rating is 5A and it is integrated with an overcurrent protection relay. In the fault location experimental system, this power supply is utilized to supply an appropriate voltage setpoint for several experiments. Secondly, the two solid-state switch modules are used to replace two circuit breakers in the system. These modules are also manufactured by Lucas Nuller, Germany. They are located at the two ends to protect when a fault occurs in the line. Besides, they can communicate with the control center via the Ethernet interface; therefore, their IP address will be set before they can receive the commands from the monitoring and controlling center. Thirdly, to measure, monitor, and control the experimental system, two PAC4200 power quality meters are also connected at the two ends of the line. These meters can measure all power quality parameters such as the frequency, voltage, current, power, etc. In addition, they can be communicated with the monitoring and controlling center via the Ethernet communication protocol, so every meter is also set to an appropriate IP address. In this experimental system, the two power quality meters continuously measure the parameters in real-time and send these parameters to the monitoring and controlling center to detect, identify, and locate accurately faults in the power transmission line. Observing Fig. 1, the current and voltage transformers are depicted to create the secondary measurement signals as the inputs of the PAC4200 power quality meters; however, all the hardware devices selected to establish this experimental system are in the laboratory range having the voltage and current ratings of 400V and 5A, respectively.

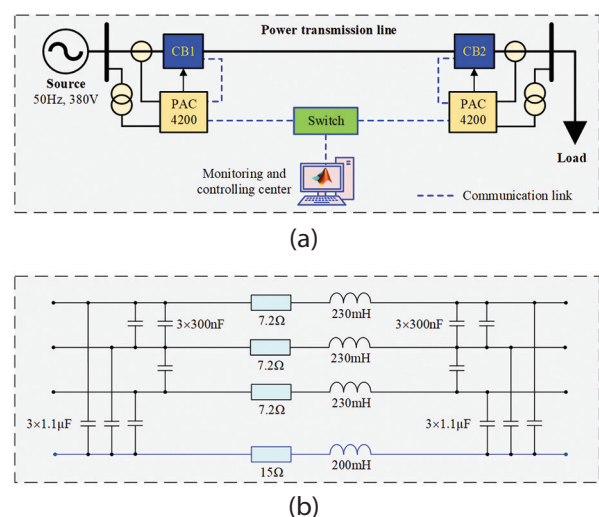


**Fig. 1.** a) The schematic diagram of the real-time fault location experimental system, b) The detail model of the transmission line

The three-phase power transmission line utilized in this experimental system is a module which is manufactured by Lucas Nuller, Germany.

This module is also designed for applications in the smart grid laboratory, and it is based on the type-Pi transmission line model as shown in Fig. 1b. The specifications of this module consist of the line length 300km, the resistance  $7.2\Omega$ , the inductance 230mH, the capacitance between phase to ground  $1.1\mu\text{F}$ , and the capacitance between phase-to-phase  $300\text{nF}$ . The real-time fault location experimental system is shown in Fig. 2.

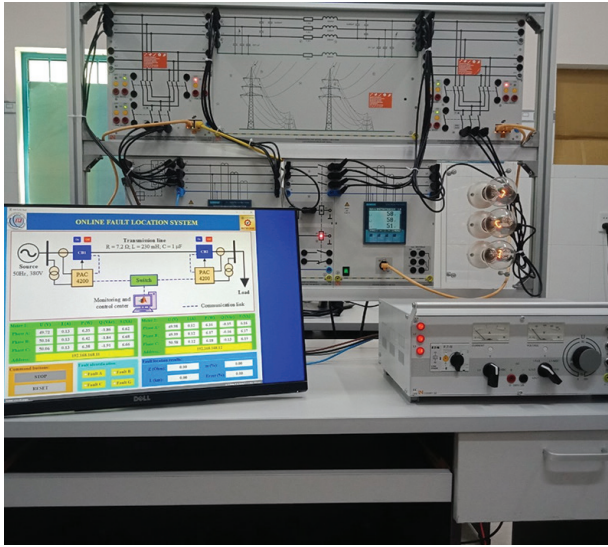


**Fig. 2.** The hardware unit of the real-time fault location experimental system

## 2.2. SOFTWARE UNIT

In this paper, the 2021a version of Matlab software was applied to design the fault location program on the transmission line. In this version, Matlab software is equipped with some advanced packages such as Modbus Explorer, App Designer, etc. Using the packages to test easily the connection between the hardware platforms and the software program. In addition, they can be used to design the friendly user guide for monitoring and controlling the fault location system. Moreover, the students can easily use the commands of Matlab to create a private program to test and record the responses of the hardware components in real-time.

The Modbus Communication toolbox of Matlab supports Modbus interaction via the TCP/IP or Serial RTU protocol. It can be used to communicate with the Modbus servers such as PLC, DSP, etc. as well as for reading data from a measurement device, controlling, and monitoring the temperature and humidity from the sensors. Besides, the coils and registers can be read by using the Modbus Explorer tool that has a friendly user guide interface. Therefore, the Modbus Explorer was used to check the read and write commands from the hardware units including: the PAC4200 power quality meters and circuit breaker modules via the Ethernet network. The user guide interface of Modbus Explorer is shown in Fig. 3. The command syntaxes in Modbus Communication are used to declare, read, and write as shown in Table 1.

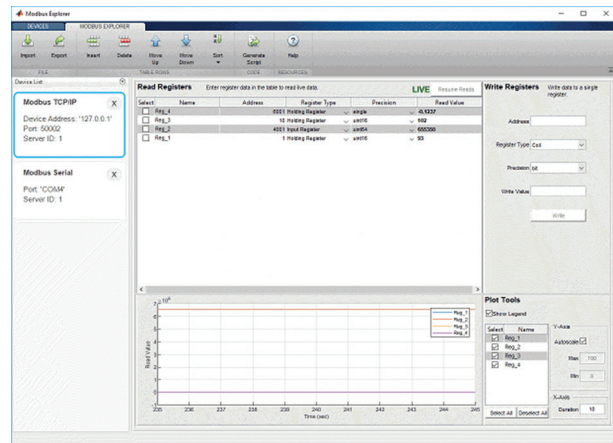


**Fig. 3.** The Modbus Explorer application to check the read and write commands

**Table 1.** The commands of Modbus Communication

Syntax	Function
modbus	Create Modbus object
read	Read data from a Modbus server
write	Perform a write operation to the connected Modbus server
writeRead	Perform a write then read operation on groups of holding registers in a single Modbus transaction
maskWrite	Perform mask write operation on a holding register
instrhwinfo	Information about available hardware
clear	Remove instrument objects from Matlab workspace

## 2.3. IMPLEMENTED ALGORITHM

The signal processing technique applied in the PAC4200 power quality meters is Discrete Fourier Transform (DFT). The voltage and current signals are sampled and processed to calculate the parameters for identifying and locating faults on the transmission line. The background of the DFT is briefed as follows [25]:

The continuous-time voltage and current signals as the inputs of the power quality meters can be defined with Fourier series representation. In addition, these discrete-time signals can be represented within finite duration in practice. An alternative transformation is called DFT for a finite-length signal, which is discretized in frequency. The frequency range of discrete-time signals is defined over the interval between  $-\pi$  to  $\pi$ . A periodic digital signal consisted of  $N$  samples is to separate the frequency components into  $2\pi/N$  radians intervals by dividing the frequency-domain. Then, Fourier series representation of the discrete-time signal will consist of  $N$  frequency components [25]. The general Fourier series representation of a periodic signal ( $x(n)$ ) is expressed as:

$$x(t) = \sum_{k=0}^{N-1} c_k e^{jk(2\pi/N)n} \quad (1)$$

where  $N$  is the harmonic index related with the exponential function ( $e^{jk(2\pi/N)n}$ ) for  $k = 0, 1, \dots, N-1$ ,  $c_k$  is the coefficients of the Fourier series.

The coefficients  $c_k$  are calculated as:

$$c_k = \frac{1}{N} \sum_{n=0}^{N-1} x(n)e^{-jk(2\pi/N)n} \quad (2)$$

The coefficients  $c^k$  of Fourier series are the form of a periodic sequence of fundamental period  $N$ . The time-domain spectrum of a periodic signal can be represented as periodic sequence with DFT. The frequency analysis of discrete-time periodic signals ( $\sin(n\tau)$  and  $\cos(n\tau)$ ) involves Fourier transform of the time-domain signal. DFT is defined as multiplication of  $N$  samples  $x(n)$  with  $N$  discrete frequencies. These samples are taken at discrete frequencies ( $\omega^k = 2\pi k/N$ ), where  $k = 0, 1, \dots, N-1$ , between  $0 \leq \omega \leq 2\pi$ . This means that  $X(\omega)$  is evaluated at the successive samples by equally spaced frequencies.  $X(\omega)$  is given in the following.

$$X(\omega_k) = \sum_{n=-\infty}^{\infty} x(n)e^{-jn(2\pi/N)kn} \quad (3)$$

DFT is a mapping between  $N$  samples  $x(n)$  of the time-domain into  $N$  samples  $X(\omega)$  of the frequency-domain. This gives the opportunity to compute DFT of the periodic and the finite-length signals. The frequency-domain spectrum of a periodic sequence can be re-obtained as the periodic signal by using inverse discrete-time Fourier transform (IDFT). IDFT can be defined by using the frequency samples of  $X(k)$ . It is given in the following.

$$X(n) = \frac{1}{N} \sum_{k=0}^{N-1} X(k)W_N^{-kn}, n = 0, 1, \dots, N-1 \quad (4)$$

IDFT shows that there is no loss information by transforming the frequency spectrum of  $X(k)$  back into the original time sequence of  $x(n)$ .

#### a) The button START

When the button START is pressed, the program will perform to get the IP addresses of the two PAC4200 meters. The program then initiates the Modbus communication, reads measurement data from the registers of the two meters via the Ethernet network, sets the read values to the user guide interface of the program. If a short circuit occurs, the current at the beginning of the line will be compared with the pickup value to send the trip command to the two circuit breakers. When the button START is pressed, the program will perform the function **STARTButtonValueChanged**(app, event) as follows:

#### **function STARTButtonValueChanged(app, event)**

```
value = app.STARTButton.Value;
if value == 1
    app.STARTButton.Text = 'STOP';
else
    app.STARTButton.Text = 'START';
end
Add_1 = app.Address1.Value;
m1 = modbus('tcpip', Add_1, 502);
Add_2 = app.Address2.Value;
```

```
m2 = modbus('tcpip', Add_2, 502);
ok = 1;
while ok == 1
Data1 = read(m1, 'holdingregs', 2, 18, 'single');
Data2 = read(m2, 'holdingregs', 2, 18, 'single');
app.Ua1.Value = Data1(1);
app.Ub1.Value = Data1(2);
app.Uc1.Value = Data1(3);
app.Ia1.Value = Data1(7);
app.Ib1.Value = Data1(8);
app.Ic1.Value = Data1(9);
app.Sa1.Value = Data1(10);
app.Sb1.Value = Data1(11);
app.Sc1.Value = Data1(12);
app.Pa1.Value = Data1(13);
app.Pb1.Value = Data1(14);
app.Pc1.Value = Data1(15);
app.Qa1.Value = Data1(16);
app.Qb1.Value = Data1(17);
app.Qc1.Value = Data1(18);
app.Ua2.Value = Data2(1);
app.Ub2.Value = Data2(2);
app.Uc2.Value = Data2(3);
app.Ia2.Value = Data2(7);
app.Ib2.Value = Data2(8);
app.Ic2.Value = Data2(9);
app.Sa2.Value = Data2(10);
app.Sb2.Value = Data2(11);
app.Sc2.Value = Data2(12);
app.Pa2.Value = Data2(13);
app.Pb2.Value = Data2(14);
app.Pc2.Value = Data2(15);
app.Qa2.Value = Data2(16);
app.Qb2.Value = Data2(17);
app.Qc2.Value = Data2(18);
value = app.STARTButton.Value;
if value == 0
    ok = 0;
    app.Notification.Text = "";
    clear m1 m2;
end
mode = app.FaultLocation.Value;
if (max(Data1(7:9)) >= 0.35) & (mode == 1)
    ok = 0;
    app.Notification.Text = "";
    clear m1 m2;
    app.m1.Value = Data1(1)/Data1(7);
    app.STARTButton.Text = 'START';
    app.STARTButton.Value = 0;
    OffCB1ButtonPushed(app, event);
    OffCB2ButtonPushed(app, event);
end
end
end
```

### b) The button STOP

The buttons STOP and START are designed by a button on the user guide interface. If the button STOP is pressed, the program will stop the while loop that is running.

### c) The button RESET

The function of the button RESET is to reset all values on the user guide interface to the initial values.

### d) The button for closing the CB1

When pressing the button ON above the circuit breaker CB1, the program will initialize the Modbus communication with the IP address of the CB1: 192.168.168.15. The program will then perform the commands to write the value 1 on the coils 1 and 5; other coils will be written with the value 0. Therefore, the circuit breaker CB1 will be closed to supply the transmission line. At that time, the color of the circuit breaker CB1 will be changed to the green color. The function **OnCB1ButtonPushed**(app, event) to close the circuit breaker CB1 at the beginning of the line as follows:

```
function OnCB1ButtonPushed(app, event)
    m_cb = modbus('tcpip', '192.168.168.15', 502);
    write(m_cb, 'coils', 1, 1)
    write(m_cb, 'coils', 2, 0)
    write(m_cb, 'coils', 3, 0)
    write(m_cb, 'coils', 4, 0)
    write(m_cb, 'coils', 5, 1)
    write(m_cb, 'coils', 6, 0)
    app.LabelCB1.BackgroundColor = 'Blue';
end
```

### e) The button for tripping the CB1

When pressing the button OFF above the circuit breaker CB1, the program will initialize the Modbus communication with the IP address of the CB1: 192.168.168.15. The program will then perform the commands to write the value 1 on the coils 1 and 6; other coils will be written with the value 0. Therefore, the circuit breaker CB1 will be tripped. At that time, the color of the circuit breaker CB1 will be changed to the red color. The function **OffCB1ButtonPushed**(app, event) to trip the circuit breaker CB1 at the beginning of the line as follows:

```
function OffCB1ButtonPushed(app, event)
    m_cb = modbus('tcpip', '192.168.168.15', 502);
    write(m_cb, 'coils', 1, 1)
    write(m_cb, 'coils', 2, 0)
    write(m_cb, 'coils', 3, 0)
    write(m_cb, 'coils', 4, 0)
    write(m_cb, 'coils', 5, 0)
    write(m_cb, 'coils', 6, 1)
    app.LabelCB1.BackgroundColor = 'Red';
end
```

### f) The button for closing the circuit breaker CB2

When pressing the button ON above the circuit breaker CB2, the program will initialize the Modbus communication with the IP address of the CB2: 192.168.168.16. The program will then perform the commands to write the value 1 on the coils 1 and 5; other coils will be written by the value 0. Therefore, the circuit breaker CB2 will be closed to supply the load. At that time, the color of the circuit breaker CB2 will be changed to the green color. The function **OnCB2ButtonPushed**(app, event) to close the circuit breaker CB2 at the ending of the line as follows:

```
function OnCB2ButtonPushed(app, event)
    m_cb = modbus('tcpip', '192.168.168.16', 502);
    write(m_cb, 'coils', 1, 1)
    write(m_cb, 'coils', 2, 0)
    write(m_cb, 'coils', 3, 0)
    write(m_cb, 'coils', 4, 0)
    write(m_cb, 'coils', 5, 1)
    write(m_cb, 'coils', 6, 0)
    app.LabelCB2.BackgroundColor = 'Blue';
end
```

### g) The button for tripping the CB2

When pressing the button OFF above the circuit breaker CB2, the program will initialize the Modbus communication with the IP address of the CB2: 192.168.168.16. The program will then perform the commands to write the value 1 on the coils 1 and 6, other coils will be written by the value 0. Therefore, the circuit breaker CB2 will be tripped. At that time, the color of the circuit breaker CB2 will be changed to the red color. The function **OffCB2ButtonPushed**(app, event) to trip the circuit breaker CB2 at the ending of the line as follows:

```
function OffCB2ButtonPushed(app, event)
    m_cb = modbus('tcpip', '192.168.168.16', 502);
    write(m_cb, 'coils', 1, 1)
    write(m_cb, 'coils', 2, 0)
    write(m_cb, 'coils', 3, 0)
    write(m_cb, 'coils', 4, 0)
    write(m_cb, 'coils', 5, 0)
    write(m_cb, 'coils', 6, 1)
    app.LabelCB2.BackgroundColor = 'Red';
end
```

The above codes are programmed in Matlab software to design and implement the fault location experimental system via the algorithm as shown in Fig. 4. All measurement data from the power meters are continuously read to calculate the fault location results when a fault occurs on the transmission line. In addition, the control buttons on the user guide are programmed by the codes in each function to run the program.

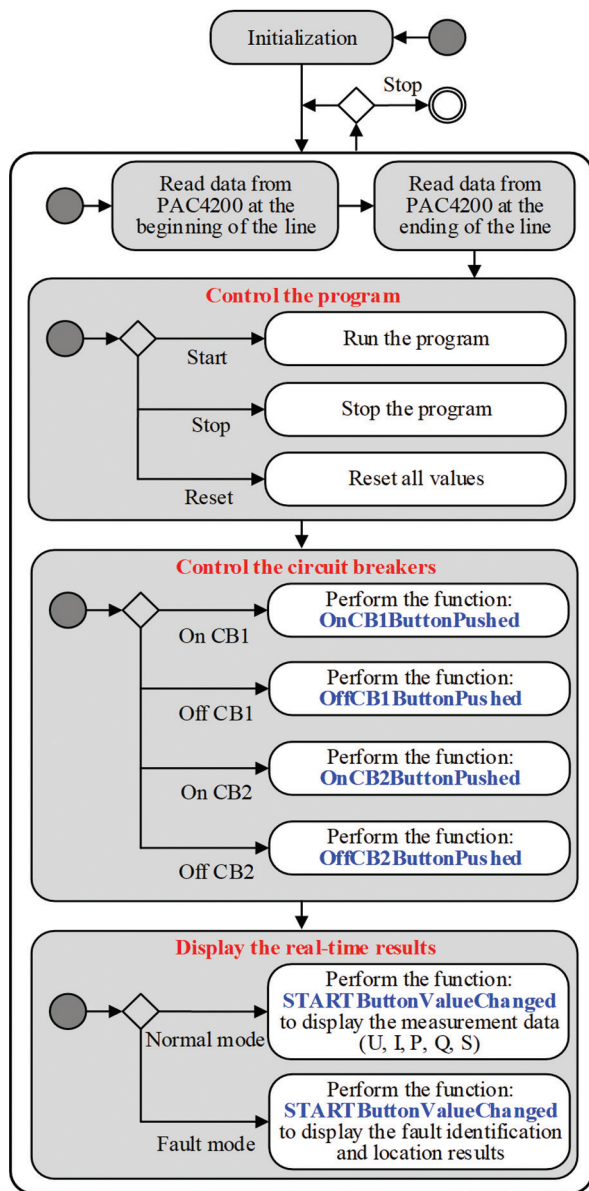


**Fig. 4.** The algorithm of the real-time fault location experimental system

The Matlab App Designer is used to design the user guide interface of the fault location program on the transmission line. After all hardware devices are correctly connected according to the diagram schematic in Fig. 1, a computer is used as a center unit to acquire and process all the signals from the hardware devices. The user guide interface of the fault location program is designed as shown in Fig. 5. The upper side of the user guide interface shows the diagram schematic and the buttons ON and OFF for closing/tripping the two circuit breakers of the transmission line. To correctly connect the program to the hardware devices of the experimental system via the Ethernet protocol, the IP addresses of the two PAC4200 power quality meters must be exactly declared on the user guide interface. In addition, the IP addresses of the two circuit breakers are established in this program. The IP addresses of the hardware devices are connected via the Ethernet protocol as shown in Table 2.

**Table 2.** The IP addresses of the hardware devices

No.	Hardware device	IP address
1	The PAC4200 power quality meter at the beginning of the line	192.168.168.11
2	The PAC4200 power quality meter at the ending of the line	192.168.168.12
3	The circuit breaker at the beginning of the line	192.168.168.15
4	The circuit breaker at the ending of the line	192.168.168.16

On the user guide interface, the open and closed statuses of the circuit breakers are remotely controlled via the On and Off. Moreover, the off and on statuses are represented by the red and green colors, respectively. The measurement data including voltage, current, active power, reactive power, and apparent power from the two PAC4200 power quality meters are continuously read in real time to display on the user guide interface. Therefore, the user can easily monitor the operation of the transmission line. In the fault mode, the center processing unit will detect and send the trip command to trip simultaneously the two circuit breakers of the line. At the same time, the fault location methods will use the measurement data from the PAC4200 meters to determine the fault location and to display the experimental results on the user guide interface.

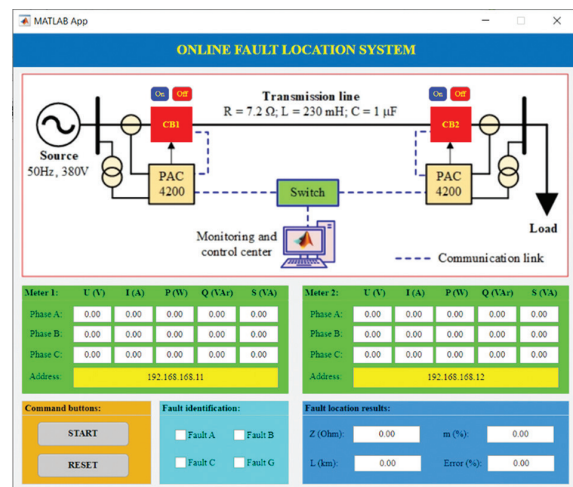


**Fig. 5.** The user guide of the program

### 3. EXPERIMENTAL RESULTS AND DISCUSSION

To carry out experiments, the hardware devices are connected according to the schematic diagram as shown in Fig. 1. The IP addresses of these power quality meters, and circuit breakers are established and communicated with the monitoring and controlling center via the Ethernet communication protocol.

#### 3.1. NORMAL OPERATION MODE WITHOUT LOAD

Controlling the circuit breakers remotely at two ends of the transmission line is performed via the buttons ON and OFF on the user guide interface. When the

program is started, the circuit is at the open status; therefore, the user allows to close the circuit breaker CB1 to supply power for the transmission line. The line is working without load and all measurement data in this case is monitored and displayed on the user guide interface as shown in Fig. 6. Observing on Fig. 6, it can be clearly seen that the currents at the PAC4200 power quality meter at the beginning of the line are  $I_A = 0.07$  A,  $I_B = 0.07$  A, and  $I_C = 0.07$  A for the phases A, B, and C respectively. These currents of three phases are due to the pi-model of the line, the reactive power of the line is injected into the system. As a result, the voltages, the currents, active powers, reactive powers, and apparent powers at the beginning of the line are shown in Fig. 6. Moreover, as the reactive power injected by the line, the voltages at the ending of the line are  $U_A = 53.92$  V,  $U_B = 53.09$  V, and  $U_C = 54.58$  V for the phases A, B, and C, respectively while the voltages at the beginning of the line are  $U_A = 50.71$  V,  $U_B = 49.89$  V, and  $U_C = 51.29$  V for the phase A, B, and C, respectively. Therefore, in this case the voltages at the ending of the line are higher than the voltages at the beginning of the line.

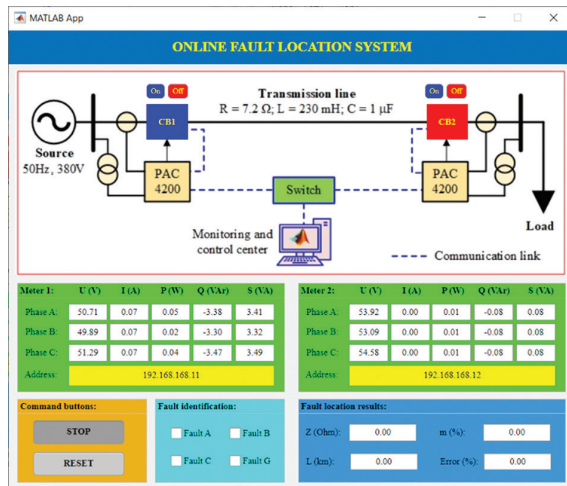


Fig. 6. The operation mode of the line without load

### 3.2. NORMAL OPERATION MODE WITH LOAD

In this mode, the circuit breaker at the ending of the line is closed to supply power to the resistance load. The load is represented by three 220 V, 60 W bulbs. The experimental results of this mode are presented in Fig. 7. It is clear that the currents at the beginning of the line ( $I_A = 0.13$  A,  $I_B = 0.13$  A, and  $I_C = 0.13$  A) and at the ending of line ( $I_A = 0.13$  A,  $I_B = 0.12$  A, and  $I_C = 0.12$  A). In addition, the active, reactive, and apparent powers are also shown in Fig. 7.

To supply the load at the ending of the transmission line, the user must close the circuit breaker CB2 at the ending of the line. The resistance loads in this case study are three 220 V, 60 W bulbs. The currents will be increased depending on the resistance loads. As a result, the monitoring results in this case are displayed in Fig. 7. From Fig. 7, the currents at the beginning of the line are

$I_A = 0.13$  A,  $I_B = 0.13$  A, and  $I_C = 0.13$  A for the phases A, B, and C, respectively and the currents at the ending of the line are  $I_A = 0.13$  A,  $I_B = 0.12$  A, and  $I_C = 0.12$  A. Besides, the active powers, reactive powers, and apparent powers are also shown on the user guide interface. For the voltages, it can be clearly seen that the voltages at the beginning of the line ( $U_A = 50.07$  V,  $U_B = 49.20$  V, and  $U_C = 50.65$  V) are higher than the voltages at the ending of the line ( $U_A = 50.10$  V,  $U_B = 49.43$  V, and  $U_C = 51.05$  V).

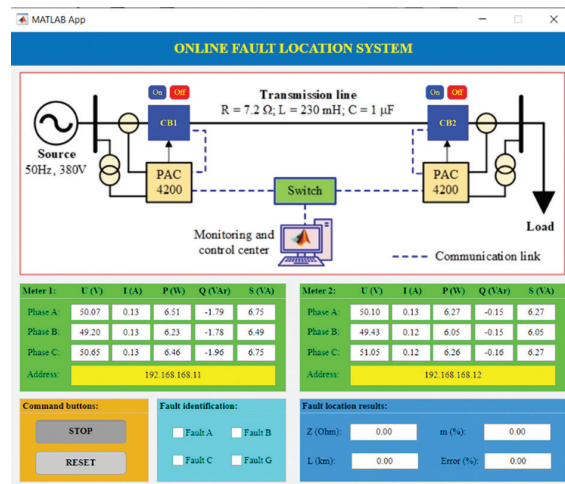


Fig. 7. The operation mode of the line with load

### 3.3. FAULT MODE

To establish faults in the experimental system, one side of a circuit breaker is connected to the ending of the line and the other side of the circuit breaker is connected to obtain several fault types including: ABCG, AB, AC, BC, AG, BG, and CG. As shown in Fig. 1, the schematic diagram of the real-time fault location experimental system consists of a type- $\pi$  transmission line model. The limitation of this experimental system is only one transmission line model; therefore, the end of the line can be only applied to investigate the performance of this system. In addition, it is assumed that the faults are solid faults with the fault resistance of  $R_F = 0\Omega$ . The experimental results for these faults are shown in the figures below.

Fig. 8 shows the monitoring, identifying, and locating experimental results when the three-phase fault ABCG at the ending of the line with the fault resistance of  $R_F = 0\Omega$ . It can be clearly seen that all measurements at the ending of the line are zero because the voltages and currents equal zero. However, the currents at the beginning of the line are the three-phase fault currents ( $I_A = 0.59$  A,  $I_B = 0.59$  A, and  $I_C = 0.59$  A). These current values are higher than the pickup value  $I_{set} = 0.25$  A; therefore, the program detects the fault and then sends the signal to trip two circuit breakers of the line (CB1 and CB2 are changed to the open status). In addition, the three-phase fault ABCG is clearly shown in the frames of fault identification and the fault location results on the user guide interface are at the location with  $m = 99.82\%$ ,  $L = 299.45$  km, and Error = -0.18%.

In this paper, two unbalanced faults including the BC fault and AG fault are created and shown in Fig. 9 and Fig. 10, respectively. The fault location results are 97.32% for the BC fault and 100.09% for the AG fault. On the other hand, the identification results and the status of the circuit breakers are displayed accurately on the user guide interface for each fault.

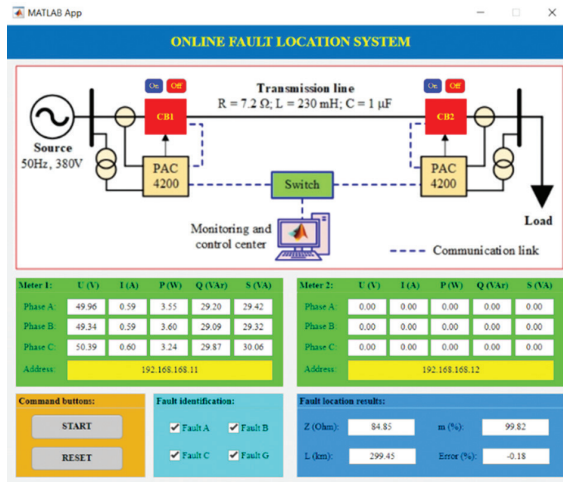


Fig. 8. The experimental result of the ABCG fault

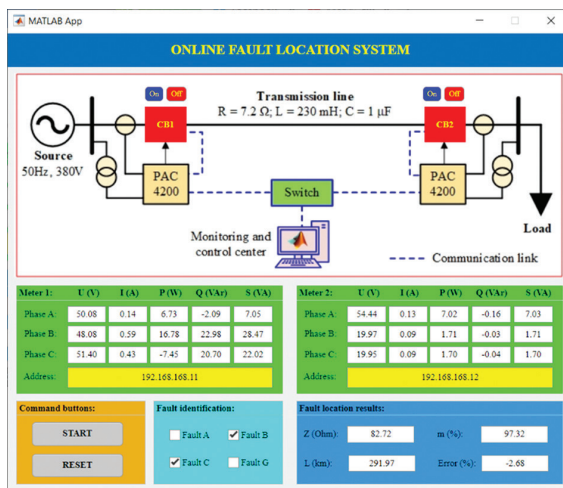


Fig. 9. The experimental result of the BC fault

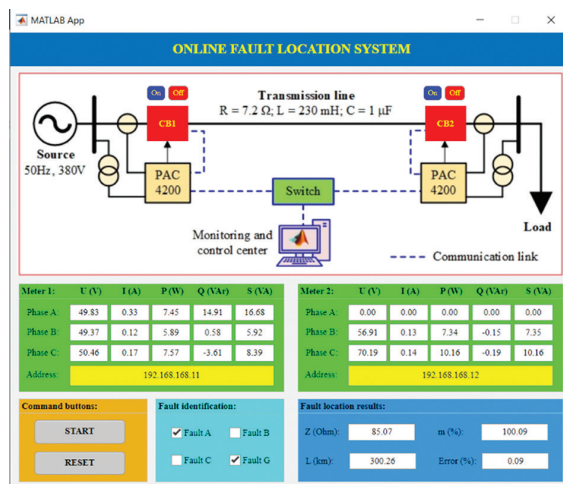


Fig. 10. The experimental result of the AG fault

The fault location results for the different fault types are also carried out in this paper and they are shown in Table 3. These experimental results confirm that the designed system can help electrical engineering students to practice with all fault types.

Table 3. The results for the different fault types

Fault type	Z ( $\Omega$ )	m%	L (km)	Error (%)
ABCG	84.85	99.82	299.45	-0.18
AB	85.02	100.02	300.07	0.02
BC	82.72	97.32	291.97	-2.68
AC	85.49	100.57	301.71	0.57
AG	85.07	100.09	300.26	0.09
BG	84.45	99.36	298.07	-0.64
CG	84.85	99.83	299.48	-0.17

#### 4. CONCLUSION

The paper presented an idea to design and implement a real-time fault location experimental system in a laboratory range. The hardware devices are connected to build an experimental system in which the type-pi three-phase power transmission line is a main device. Furthermore, the real-time measurement data is continuously monitored at the monitoring and controlling center via the Ethernet communication protocol. The software program with the friendly user guide interface is designed to detect, identify, and locate faults that occur in the power transmission line. The main function of the experimental system is to train the electrical engineering students in how to understand the fault location issue in real power systems.

For future works, the authors will develop the experimental system by additional functions such as varying the fault locations as well as the fault resistances along the line. Machine learning and artificial intelligence methods will be applied in the software unit of the experimental system to help students approach these methods.

#### 5. REFERENCES:

- [1] S. Das, S. Santoso, A. Gaikwad, M. Patel, "Impedance-based fault location in transmission networks: theory and application", IEEE Access, Vol. 2, 2017, pp. 537-557.
- [2] Y. J. Deng, C. M. Wang, S. Zhang, W. Z. Han, "A fault location algorithm for shunt-compensated lines under dynamic conditions", International Journal of Electrical Power & Energy Systems, Vol. 143, 2022, pp. 108387.
- [3] R. Fan, Y. Liu, R. Huang, R. Diao, S. Wang, "Precise Fault Location on Transmission Lines Using Ensemble Kalman Filter", IEEE Transactions on Power Delivery, Vol. 33, No. 6, 2018, pp. 3252-3255.



- [4] F. V. Lopes, E. J. S. Leite Jr, J. P. G. Ribeiro, A. B. Piardi, A. V. Scheid, G. Zat, R. G.F. Espinoza, "Single-ended multi-method phasor-based approach for optimized fault location on transmission lines", *Electric Power Systems Research*, Vol. 212, 2022, p. 108361.
- [5] C. M. Furse, M. Kafal, R. Razzaghi, Y.-J. Shin, "Fault diagnosis for electrical systems and power networks: A review", *IEEE Sensors Journal*, Vol. 21, No. 2, 2020, pp. 888-906.
- [6] A. N. Sheta, G. M. Abdulsalam, A. A. Eladl, "Online tracking of fault location in distribution systems based on PMUs data and iterative support detection", *International Journal of Electrical Power & Energy Systems*, Vol. 128, 2021, p. 106793.
- [7] A. Gopalakrishnan, M. Kezunovic, S. M. McKenna, D. M. Hamai, "Fault location using the distributed parameter transmission line model", *IEEE Transactions on Power Delivery*, Vol. 15, No. 4, 2000, pp. 1169-1174.
- [8] S. S. Gururajapathy, H. Mokhlis, H. A. Illias, "Fault location and detection techniques in power distribution systems with distributed generation: A review", *Renewable and Sustainable Energy Reviews*, Vol. 74, 2017, pp. 949-958.
- [9] Y. Jia, Y. Liu, B. Wang, D. Lu, Y. Lin, "Power Network Fault Location with Exact Distributed Parameter Line Model and Sparse Estimation", *Electric Power Systems Research*, 2022, p. 108137. (in press)
- [10] S. M. Saad, N. El Nailly, F. A. Mohamed, "Investigating the effect of DG infeed on the effective cover of distance protection scheme in mixed-MV distribution network", *International Journal of Renewable Energy Development*, Vol. 7, No. 3, 2018, pp. 223-231.
- [11] A. Swetapadma, S. Chakrabarti, A. Y. Abdelaziz, "Feasibility study of intelligent fault location estimation methods for double-circuit transmission lines", *International Transactions on Electrical Energy Systems*, Vol. 31, No. 12, 2021, p. e13198.
- [12] Z. Han, S. Li, S. Liu, S. Gao, "A reactance-based fault location method for overhead lines of AC electrified railway", *IEEE Transactions on Power Delivery*, Vol. 35, No. 5, 2020, pp. 2558-2560.
- [13] T. Namas, I. Džafić, "Least square method for impedance based fault location in ungrounded networks", *Proceedings of the 2<sup>nd</sup> Global Power, Energy and Communication Conference*, Izmir, Turkey, 20-23 October 2020, pp. 274-278.
- [14] J. Barati, A. Doroudi, "Novel modified impedance-based methods for fault location in the presence of a fault current limiter", *Turkish Journal of Electrical Engineering & Computer Sciences*, Vol. 26, No. 4, 2018, pp. 1881-1893.
- [15] K. Kalita, S. Anand, S. K. Parida, "A novel non-iterative fault location algorithm for transmission line with unsynchronized terminal", *IEEE Transactions on Power Delivery*, Vol. 36, No. 3, 2021, pp. 1917-1920.
- [16] C. A. Apostolopoulos, C. G. Arsoniadis, P. S. Georgilakis, V. C. Nikolaidis, "Fault location algorithms for active distribution systems utilizing two-point synchronized or unsynchronized measurements", *Sustainable Energy, Grids and Networks*, Vol. 32, 2022, p. 100798.
- [17] F. Xu, X. Dong, "A novel single-ended traveling wave fault location method based on reflected wave-head of adjacent bus", *Proceedings of the 12<sup>th</sup> IET International Conference on Developments in Power System Protection*, Copenhagen, Denmark, 31 March - 03 April 2014, pp. 1-5.
- [18] J. Xie, G. Jin, Y. Wang, X. Ni, X. Liu, "New Algorithm for 2-terminal Transmission Line Fault Location Integrating Voltage Phasor Feature and Phase Angle Jump Checking", *Electric Power Systems Research*, Vol. 209, 2022, p. 10797.
- [19] M. Majidi, M. Etezadi-Amoli, "A new fault location technique in smart distribution networks using synchronized/ nonsynchronized measurements", *IEEE Transactions on Power Delivery*, Vol. 33, No. 3, 2017, pp. 1358-1368.
- [20] J. Liang, T. Jing, H. Niu, J. Wang, "Two-terminal fault location method of distribution network based on adaptive convolution neural network", *IEEE Access*, Vol. 8, 2020, pp. 54035-54043.
- [21] M.-R. Mosavi, A. Tabatabaei, "Traveling-wave fault location techniques in power system based on wavelet analysis and neural network using GPS timing", *Wireless Personal Communications*, Vol. 86, No. 2, 2016, pp. 835-850.

- [22] R. L. A. Reis, F. V. Lopes, W. L. A. Neves, D. Fernandes Jr., C. M. S. Ribeiro, G. A. Cunha, "An improved single-ended correlation-based fault location technique using traveling waves", *International Journal of Electrical Power & Energy Systems*, Vol. 132, 2021, p. 107167.
- [23] S. Sawai, R. N. Gore, O. D. Naidu, "Novel traveling wave phase component-based fault location of transmission lines", *Proceedings of the IEEE International Conference on Power Electronics, Drives and Energy Systems*, Jaipur, India, 16-19 December 2020, pp. 1-5.
- [24] H. Shu, X. Liu, X. Tian, "Single-Ended Fault Location for Hybrid Feeders Based on Characteristic Distribution of Traveling Wave Along a Line", *IEEE Transactions on Power Delivery*, Vol. 36, No. 1, 2021, pp. 339-350.
- [25] S. M. Kuo, B. H. Lee, "Real-time digital signal processing implementations applications and experiments with the TMS320C55x", John Wiley & Sons, 2001.